ARTICLE IN PRESS

Available online at www.sciencedirect.com

SCIENCE DIRECT

Robotics and Autonomous Systems ▮ (▮▮▮▮) ▮▮▮–▮▮▮

Robotics and Autonomous Systems

www.elsevier.com/locate/robot

Trajectory tracking control of farm vehicles in presence of sliding

H. Fang[a,*], Ruixia Fan[a], B. Thuilot[b], P. Martinet[b]

[a] *Beijing Institute of Technology, 100081, Beijing, China*
[b] *LASMEA, 24, av. des Landais, 63177 Aubiere Cedex, France*

Received 8 March 2005; accepted 26 April 2006

Abstract

In automatic guidance of agriculture vehicles, lateral control is not the only requirement. Much research work has been focused on trajectory tracking control which can provide high longitudinal-lateral control accuracy. Satisfactory results have been reported as soon as vehicles move without sliding. But unfortunately pure rolling constraints are not always satisfied especially in agriculture applications where working conditions are rough and not predictable. In this paper the problem of trajectory tracking control of autonomous farm vehicles in the presence of sliding is addressed. To take sliding effects into account, three variables which characterize sliding effects are introduced into the kinematic model based on geometric and velocity constraints. With a linearized approximation, a refined kinematic model is obtained in which sliding effects appear as additive unknown parameters to the ideal kinematic model. By an integrating parameter adaptation technique with a *backstepping method*, a stepwise procedure is proposed to design a robust adaptive controller in which time-invariant sliding is compensated for by parameter adaptation and time-varying sliding is corrected by a Variable Structure Controller (VSC). It is theoretically proven that for farm vehicles subjected to sliding, the longitudinal-lateral deviations can be stabilized near zero and the orientation errors converge into a neighborhood near the origin. To be more realistic for agriculture applications, an adaptive controller with projection mapping is also proposed. Both simulation and experimental results show that the proposed (robust) adaptive controllers can guarantee high trajectory tracking accuracy regardless of sliding.

Keywords: Trajectory tracking control; Nonholonomic systems; Backstepping; Robust control

1. Introduction

Automatic guidance of farm vehicles develops with the requirement of modern agriculture. High-precision agriculture becomes a reality especially thanks to new localization technologies such as GPS, laser range scans and sonar. In agriculture fields it is quite common that several vehicles (including cropping, threshing, cleaning, seeding and spraying machines) compose a platoon for combined harvesting. In this case driving safety requiring constant longitudinal distances between the leading vehicle and following vehicles is an additional requirement along with the effort of improving lateral path-following performances. Therefore vehicle motions are specified not only by a geometric path but also by a time law with respect to the longitudinal direction. Since longitudinal-lateral control becomes more and more important, many research teams have paid their attention to trajectory tracking control, satisfactory results have been reported as soon as vehicles satisfy pure rolling constraints [1–7].

However due to various factors such as slipping of tires, deformability or flexibility of wheels, pure rolling constraints are never strictly satisfied. Especially in agriculture applications when farm vehicles are required to move on all-terrain grounds including slippery slopes, sloppy grass grounds, sandy and stony grounds, sliding inevitably occurs which deteriorates automatic guidance performance and even system stability.

Until now there are very few papers dealing with sliding. [8] prevents cars from skidding by robust decoupling of car steering dynamics, but acceleration measurements are necessary and the steering angle is assumed small. [10] copes with the control of WMR (Wheeled Mobile Robot) not satisfying the ideal kinematic constraints by using slow manifold methods, but the parameters characterizing the sliding effects are assumed to be exactly known. Therefore [8,10] are

* Corresponding address: 1-20-505 Xi'an Jiaotong University, 710049 Xi'an, China. Fax: +86 10 68913261.
E-mail address: fangqx@mail.xjtu.edu.cn (H. Fang).

0921-8890/$ - see front matter
doi:10.1016/j.robot.2006.04.011

not realistic for agriculture applications. In [11] a controller is designed based on the averaged model allowing the tracking errors to converge to a limit cycle near the origin. In [15] a general singular perturbation formulation is developed which leads to robust results for linearizing feedback laws ensuring trajectory tracking. But above two schemes only take into account sufficiently small sliding effects and they are too complicated for real-time practical implementation. In [12, 13] Variable Structure Control (VSC) is used to eliminate the harmful sliding effects when the bounds of the sliding effects have been known. The trajectory tracking problem of mobile robots in the presence of sliding is solved in [14] by using discrete-time sliding mode control. But the controllers [12–14] counteract sliding effects **only** relying on high-gain controllers which is not realistic because of limited bandwidth and low level delay introduced by steering systems of farm vehicles. In [16] sliding effects are rejected by re-scheming desired paths adaptively based on steady control errors which are mainly caused by modeled sliding effects. Moreover a robust adaptive controller is designed in [17] which can compensate sliding by parameter adaptation and VSC. But [16,17] only care about lateral control.

In the references referred above most research works treated sliding as disturbances, but alternatively sliding can be also regarded specifically as time-varying parameters. On the other hand backstepping methods which are used widely in controller design have been proven powerful in controlling nonholonomic systems with uncertain parameters [18,21]. With this idea in our previous work [17] we have applied backstepping successfully to design an anti-sliding lateral controller. The purpose of this paper is to extend our lateral controller to a practical longitudinal-lateral controller in presence of sliding.

The main idea of this paper is that sliding effects are introduced as additive unknown parameters to the ideal kinematic model, based on *backstepping method* a robust adaptive controller is designed. Furthermore to be of benefit to actual applications the robust adaptive controller is simplified into an adaptive controller with projection mapping. This paper is organized as follows, in Section 2 a kinematic model considering sliding is constructed in the vehicle body frame. In Section 3 for an ideal kinematic model a trajectory tracking controller is designed. In Section 4 a robust adaptive controller is designed in presence of sliding by using backstepping methods. In Section 5 the robust adaptive controller is simplified into an adaptive controller with projection mapping. In Section 6, some comparative simulation and experimental results are presented to validate the proposed control laws.

2. Kinematic model for trajectory tracking control

2.1. Notation and problem description

In this paper the vehicle is simplified by a bicycle model, the kinematic model is expressed in the vehicle body frame (o, x', y') (see Fig. 1). Necessary variables appearing in the kinematic model are denoted as follows:

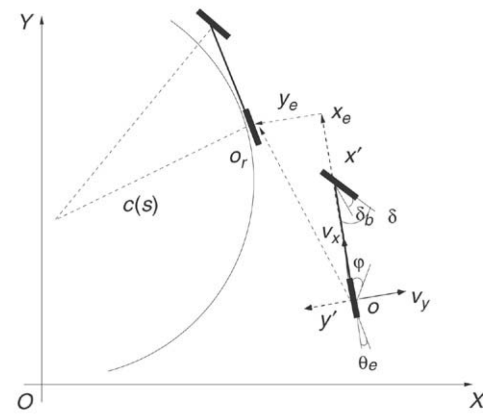

Fig. 1. Notations of the kinematic model.

- o (o_r) is the center of the (reference) vehicle virtual rear wheel.
- x' is the vector corresponding to the vehicle body centerline
- y' is the vector vertical to x'.
- (x_r, y_r) are the coordinates of the reference point o_r with respect to the inertia frame.
- (x, y) are the coordinates of the vehicle o with respect to the inertia frame.
- (x_e, y_e) depict the vector $\overrightarrow{oo_r}$ in the vehicle body frame (o, x', y').
- $c(s)$ is the curvature of the path, s is the curvilinear coordinates (arc-length) of the point o_r along the reference path from an initial position.
- θ (θ_r) is the orientation of the (reference) vehicle centerline with respect to the inertia frame.
- $\theta_e = \theta_r - \theta$ is the orientation error.
- l is the vehicle wheelbase.
- v (v_r) is the linear velocity of the (reference) vehicle with respect to the inertia frame.
- v_ω is the rear wheel rotating velocity.
- v_x is the longitudinal velocity of the vehicle in the direction of ox' w.r.t the inertia frame.
- v_y is the lateral velocity of the vehicle in the direction of oy' w.r.t the inertia frame.
- δ is the steering angle of the virtual front wheel.
- δ_b is the steering angle bias due to sliding.

So the trajectory tracking errors can be described by (x_e, y_e, θ_e). The driving velocity of the rear wheel v_ω and the steering angle of the front wheel δ are two control inputs. The aim of this paper is to design a controller (v_ω, δ) which can guarantee the longitudinal-lateral errors x_e, y_e approach to zero and the orientation error θ_e is bounded in presence of sliding.

2.2. Kinematic model

From Fig. 1, it is easy to obtain the following geometric relationship

$$\begin{pmatrix} x_e \\ y_e \\ \theta_e \end{pmatrix} = \begin{pmatrix} \cos\theta & \sin\theta & 0 \\ -\sin\theta & \cos\theta & 0 \\ 0 & 0 & 1 \end{pmatrix} \begin{pmatrix} x_r - x \\ y_r - y \\ \theta_r - \theta \end{pmatrix} \tag{1}$$

and the velocity constraint

$$\begin{cases}\dot{x} = v\cos\theta \\ \dot{y} = v\sin\theta.\end{cases} \tag{2}$$

In this paper it is assumed that $|\theta_e| < \frac{\pi}{2}$. When vehicles move without sliding (v is equivalent to v_x), the angular velocity can be expressed by

$$\dot{\theta} = \omega = \frac{v}{l}\tan\delta. \tag{3}$$

The angular velocity of the reference vehicle is

$$\dot{\theta}_r = \frac{v_r}{\frac{1}{c(s)}}. \tag{4}$$

The ideal kinematic model with respect to (o, x', y') can be developed directly by differentiating (1) (see Appendix A for details)

$$\begin{cases}\dot{x}_e = -v + v_r\cos\theta_e + \omega y_e \\ \dot{y}_e = v_r\sin\theta_e - \omega x_e \\ \dot{\theta}_e = v_r c(s) - \dfrac{v}{l}\tan\delta.\end{cases} \tag{5}$$

But when vehicles move on a steep slope or the ground is slippery, sliding occurs inevitably. Moreover in actual agriculture applications, the vehicles have horizontal reactions (harvesting, tilling) from the end-effectors, which makes longitudinal sliding serious. So (5) is no longer valid, the violation of the pure rolling constraints is described by introducing three sliding parameters, which are the longitudinal sliding velocity v_x^s, the lateral sliding velocity v_y^s and bias of the steering angle δ_b. Among them the measurement of v_x^s can be obtained relatively accurately under actual low S/N ratio conditions by considering the difference between the wheel rotating velocity and the vehicle moving speed. While v_y^s and δ_b cannot be measured precisely because in comparison with their values, the GPS measurement noises and the external disturbances become rather important. So in this paper we treat v_x^s as a known parameter, v_y^s and δ_b are regarded as two unknown variables which will be corrected by means of robust adaptive controller design.

The longitudinal-lateral velocities in presence of sliding satisfy the following constraints

$$\begin{cases}v_x = v_\omega + v_x^s \\ v_y = v_y^s\end{cases} \tag{6}$$

and the vehicle angular velocity becomes

$$\omega = \frac{v_x}{l}\tan(\delta + \delta_b) - \frac{v_y}{l}. \tag{7}$$

Therefore the velocity constraints (2) become

$$\begin{cases}\dot{x} = v\cos(\theta + \varphi) \\ \dot{y} = v\sin(\theta + \varphi)\end{cases} \tag{8}$$

where

$$v = \sqrt{v_x^2 + v_y^2} \tag{9}$$

and φ is the side sliding angle defined by

$$\varphi = \arctan\left(\frac{v_y}{v_x}\right). \tag{10}$$

By using the similar method the kinematic model when sliding is taken into account is obtained (see Appendix B for details)

$$\begin{cases}\dot{x}_e = -v_x + v_r\cos\theta_e + \omega y_e \\ \dot{y}_e = -v_y + v_r\sin\theta_e - \omega x_e \\ \dot{\theta}_e = v_r c(s) - \left(\dfrac{v_x}{l}\tan(\delta + \delta_b) - \dfrac{v_y}{l}\right).\end{cases} \tag{11}$$

Note that

$$v_x = v\cos\varphi \tag{12}$$

is the longitudinal velocity. In the case when no sliding occurs, it is obvious that $v_x = v_\omega = v$.

2.3. Kinematic model with linearization approximation

In actual agriculture applications, it is general that the ground conditions (gradient, friction, curvature) do not change abruptly and most trajectories to be tracked are straight lines and circles. So when farm vehicles move smoothly without too much acceleration, it is reasonable to assume that the sliding parameters vary not too greatly with time, the sliding effects can be described by

$$\begin{aligned}v_y^s &= \bar{v}_y + \varepsilon_1 \\ \delta_b &= \bar{\delta}_b + \varepsilon_2'\end{aligned} \tag{13}$$

where $\bar{v}_y$, $\bar{\delta}_b$ are time-invariant (other complicated working conditions for example the vehicle traverses side slopes in both directions are not considered, they will be addressed in future works), ε_1, ε_2' are time-varying variables with zero mean value. Furthermore since the steering bias δ_b is quite small (In our experiments its value varies within the range of [0, 5] degree), the orientation kinematic equation of (11) can be linearized resulting in trivial errors. Therefore the kinematic model (11) is rewritten as

$$\dot{x}_e = -(v_\omega + v_x^s) + v_r\cos\theta_e + \omega y_e \tag{14a}$$

$$\dot{y}_e = v_r\sin\theta_e - \omega x_e - (\bar{v}_y + \varepsilon_1) \tag{14b}$$

$$\dot{\theta}_e = c(s)v_r + \frac{\bar{v}_y + \varepsilon_1}{l} - \frac{v_\omega + v_x^s}{l}(\tan\delta + \tan\bar{\delta}_b + \varepsilon_2) \tag{14c}$$

where $\varepsilon_2 = \tan\varepsilon_2' + \epsilon$, ϵ is the error due to linearization approximation.

Note that the wheel rotating velocity v_ω and the steering angle of the front wheel δ are two control inputs to be designed.

3. Backstepping-based control design for ideal kinematic model

3.1. Application of backstepping-based control to nonholonomic systems

It is well known that nonholonomic systems cannot be stabilized by smooth static state feedback laws [22]. Presently the widely used control methods are such classical means that control nonholonomic systems in cascaded forms. Among them chained system theories [9] and backstepping schemes [2,4] are the most important nonlinear control skills with numerous applications.

Here we turn to [5] to illustrate general knowledge about backstepping control schemes and its applications to nonholonomic systems by means of a simple example considering the special case of integrator backstepping. For a more detailed explanation the reader is referred to [19,20].

Consider the second order system

$$\dot{x} = \cos x - x^3 + \xi \tag{15a}$$

$$\dot{\xi} = u \tag{15b}$$

where $[x, \xi]^T \in R^2$ is the state and u is the input. We want to design a state-feedback controller to render the equilibrium point $[x, \xi]^T = [0, -1]^T$ globally asymptotically stable.

If ξ were the input, then (15a) can easily be stabilized by means of $\xi = -\cos x - c_1 x$. A Lyapunov function would be $V(x) = \frac{1}{2}x^2$.

Unfortunately ξ is not the control input but a state variable. Nevertheless, we could prescribe its desired value by

$$\xi_d = -\cos x - c_1 x. \tag{16}$$

Next we define z to be the difference between ξ and its desired value:

$$z = \xi - \xi_d = \xi + \cos x + c_1 x. \tag{17}$$

We can now write the system (15) in the new co-ordinates $(x; z)$

$$\begin{aligned} \dot{x} &= -c_1 x - x^3 + z \\ \dot{z} &= u + (c_1 - \sin x)(-c_1 x - x^3 + z). \end{aligned} \tag{18}$$

To obtain a Lyapunov function candidate we simply augment the Lyapunov function with a quadratic term in z:

$$V_a(x, \xi) = V(x) + \frac{1}{2}z^2 = \frac{1}{2}x^2 + \frac{1}{2}(\xi + \cos x + c_1 x)^2. \tag{19}$$

The derivative of V_a along the solutions of (18) becomes

$$\begin{aligned} \dot{V}_a &= -c_1 x^2 - x^4 \\ &\quad + z(x + u + (c_1 - \sin x)(-c_1 x - x^3 + z)). \end{aligned} \tag{20}$$

The simplest way to arrive at a negative definite $\dot{V}_a$ is to choose

$$u = -c_2 z - x - (c_1 - \sin x)(-c_1 x - x^3 + z) \tag{21}$$

which in the original co-ordinates $[x; \xi]^T$ becomes

$$\begin{aligned} u &= -(c_1 + c_2)\xi - (1 + c_1 c_2)x - (c_1 + c_2)\cos x \\ &\quad + c_1 x^3 - x^3 \sin x + \xi \sin x + \sin x \cos x. \end{aligned} \tag{22}$$

Usually ξ is called a virtual control.

One of the advantages of backstepping is that it provides a constructive systematic method to arrive at globally stabilizing control laws. Unfortunately, one usually obtains complex expressions (in the original co-ordinates) for the control law, as already can be seen from (22).

3.2. *Trajectory tracking control for ideal kinematic model*

First the ideal kinematic model without sliding is considered. Notice that (5) is a 2–3 nonholonomic system in which y_e is not directly controlled. To overcome this problem the idea of backstepping is used. Using backstepping we propose a stepwise design procedure for this 3-order nonholonomic system. Due to limited space, we present the design scheme briefly.

Step 1: Considering the ideal kinematic model (5) where $v = v_x = v_\omega$, we choose the Lyapunov function candidate for the first step as

$$V_1 = \frac{1}{2}x_e^2 + \frac{1}{2}y_e^2. \tag{23}$$

The derivative of V_1 along (5) is

$$\dot{V}_1 = x_e(-v_\omega + v_r \cos\theta_e) + y_e v_r \sin\theta_e \tag{24}$$

where two terms of ωx_e and ωy_e have disappeared because of algebraic simplification. Regard $u_1 = \sin\theta_e$ as the virtual control input of the first step. If choose u_1 as

$$u_{1d} = \frac{-k_y y_e}{v_r} \tag{25}$$

and

$$v_\omega = v_r \cos\theta_e + k_x x_e \tag{26}$$

then we have

$$\dot{V}_1 = -k_x x_e^2 - k_y y_e^2. \tag{27}$$

So u_{1d} of (25) is the desired value of the virtual control input u_1 for the first step. If u_1 tracks (25) precisely, then the longitudinal and lateral deviations will converge to zero asymptotically.

Indeed in the closed loop system u_1 is not the actual control input, tracking u_{1d} with some errors, therefore $\tilde{u}_1$ is defined as

$$\tilde{u}_1 = u_1 - u_{1d}. \tag{28}$$

Computing the time derivative of $\tilde{u}_1$ yields

$$\dot{\tilde{u}}_1 = \cos\theta_e(c(s)v_r - \omega) + \frac{k_y}{v_r}(v_r \sin\theta_e - \omega x_e). \tag{29}$$

Step 2: Consider the Lyapunov function as

$$V_2 = V_1 + \frac{1}{2}\tilde{u}_1^2. \tag{30}$$

Then the time derivative of V_2 along (24) and (29) is

$$\begin{aligned} \dot{V}_2 &= x_e(-v_\omega + v_r \cos\theta_e) + y_e v_r u_1 \\ &\quad + \tilde{u}_1\left(\cos\theta_e v_r c(s) - \left(\cos\theta_e + \frac{k_y x_e}{v_r}\right)\omega + k_y \sin\theta_e\right). \end{aligned} \tag{31}$$

After substituting (25), (26) and (28) into (31), the following equation can be deduced

$$\begin{aligned} \dot{V}_2 &= -k_x x_e^2 - k_y y_e^2 + \tilde{u}_1\Bigg(y_e v_r + \cos\theta_e v_r c(s) \\ &\quad - \left(\cos\theta_e + \frac{k_y x_e}{v_r}\right)\omega + k_y \sin\theta_e\Bigg). \end{aligned} \tag{32}$$

In (32) if ω is chosen as

$$\omega = \frac{y_e v_r + \cos\theta_e v_r c(s) + k_y \sin\theta_e + k_u \tilde{u}_1}{\cos\theta_e + \frac{k_y x_e}{v_r}} \tag{33}$$

where

$$\tilde{u}_1 = \sin\theta_e + \frac{k_y y_e}{v_r}. \tag{34}$$

Then we can obtain

$$\dot{V}_2 = -k_x x_e^2 - k_y y_e^2 - k_u \tilde{u}_1^2. \tag{35}$$

So for the ideal kinematic model without sliding the resulting control laws are

$$v_\omega = v_r \cos\theta_e + k_x x_e \tag{36}$$

$$\begin{aligned}\delta &= \arctan\left(\frac{l\omega}{v_\omega}\right)\\ &= \arctan\left(\frac{l}{v_\omega}\frac{y_e v_r + \cos\theta_e v_r c(s) + k_y \sin\theta_e + k_u \tilde{u}_1}{\cos\theta_e + \frac{k_y x_e}{v_r}}\right)\end{aligned} \tag{37}$$

where $(k_x, k_y, k_u) \in R^{+3}$. We refer interested readers to [26] for details.

3.3. Stability analysis

(35) indicates the stability of the closed-loop system. The direct application of LaSalle invariance principle yields that all the solutions converge to the set Ω with

$$\Omega = \{(x_e, y_e, \tilde{u}_1) : x_e = 0, y_e = 0, \tilde{u}_1 = 0\}. \tag{38}$$

In Ω one gets $\frac{-k_y y_e}{v_r} = \sin\theta_e$. Moreover when the lateral deviation converges to zero, simultaneously the steady orientation error θ_e converges to zero also. Therefore when vehicles move without sliding, the proposed controller can stabilize the closed-loop system to zero.

4. Backstepping-based trajectory tracking control in presence of sliding

4.1. Robust adaptive control for kinematic model with sliding

Consider the kinematic model (14). It is a 2–3 nonholonomic system with unknown constant parameters $\bar{v}_y$, $\bar{\delta}_b$ and time-varying disturbances ε_i. In this paper it is assumed that ε_i is bounded by

$$|\varepsilon_i| < \rho_i. \tag{39}$$

So we are in the position to design a controller which not only can estimate and compensate unknown parameters but also is robust to ε_i.

Step 1: Consider the sub-kinematic equations (14a) and (14b). The Lyapunov function candidate is chosen as

$$V_1 = \frac{1}{2}x_e^2 + \frac{1}{2}y_e^2 + \frac{1}{2}(\hat{\bar{v}}_y - \bar{v}_y)^T \Gamma^{-1}(\hat{\bar{v}}_y - \bar{v}_y) \tag{40}$$

where Γ is positive definite, $\hat{\bar{v}}_y$ indicates the estimation of $\bar{v}_y$. The time derivative of V_1 along the kinematic model is

$$\begin{aligned}\dot{V}_1 &= x_e(-v_\omega - v_x^s + v_r\cos\theta_e) + y_e(v_r \sin\theta_e\\ &\quad - \hat{\bar{v}}_y - \varepsilon_1) + (\hat{\bar{v}}_y - \bar{v}_y)^T\Gamma^{-1}(\dot{\hat{\bar{v}}}_y + \Gamma y_e)\end{aligned} \tag{41}$$

where two terms of ωx_e and ωy_e have disappeared after algebraic simplification. Regard $u_1 = \sin\theta_e$ as the virtual control input of the first step. If we choose u_1 as a variable structure controller

$$u_{1d} = \frac{-k_y y_e + \hat{\bar{v}}_y - \rho_1 \operatorname{sign}(y_e)}{v_r} \tag{42}$$

and let

$$v_\omega = v_r\cos\theta_e + k_x x_e - v_x^s \tag{43}$$

$$\dot{\hat{\bar{v}}}_y = -\Gamma y_e \tag{44}$$

then we have

$$\dot{V}_1 < -k_x x_e^2 - k_y y_e^2 - (\rho_1 - |\varepsilon_1|)|y_e|. \tag{45}$$

So u_{1d} of (42) is the desired value of the virtual control input u_1 for the first step. If u_1 tracks (42) precisely, then the longitudinal and lateral deviations will converge to zero asymptotically.

Indeed in the closed loop system u_1 is not the actual control input, tracking u_{1d} with some errors, therefore $\tilde{u}_1$ is defined as

$$\tilde{u}_1 = u_1 - u_{1d}. \tag{46}$$

In backstepping procedures the time differential of control laws is required, therefore backstepping schemes can be applied only to continuous kinematic control laws. In this backstepping schemes the derivative of u_{1d} must appear in the following steps, but sign() included in (42) is not differentiable. Furthermore the sign() function may cause too much oscillations (chattering) when the response time delay is considered. So in the following parts of this paper, sign() is replaced by tanh() which is continuously differentiable. Therefore u_{1d} becomes

$$u_{1d} = \frac{-k_y y_e + \hat{\bar{v}}_y - \rho_1 \tanh(\frac{y_e}{\sigma_1})}{v_r} \tag{47}$$

where $\sigma_1 > 0$.

In (41) letting $\sin\theta_e$ equal (47) instead of (42) and considering (43), (44), we have

$$\dot{V}_1 < -k_x x_e^2 - k_y y_e^2 - (\rho_1 - |\varepsilon_1|)|y_e| + \zeta_1 \tag{48}$$

where ζ_1 is a trivial variation due to the replacement of sign() by tanh() in (42).

Substituting (47) into (46) and computing the time derivative yields (see Appendix C for details)

$$\begin{aligned}\dot{\tilde{u}}_1 &= \cos\theta_e\left(c(s)v_r + \frac{\bar{v}_y + \varepsilon_1}{l} - \frac{v_\omega + v_x^s}{l}(\tan\delta + \eta + \varepsilon_2)\right)\\ &\quad + \frac{1}{v_r}(\varpi\,\dot{y}_e - \dot{\hat{\bar{v}}}_y)\end{aligned} \tag{49}$$

where

$$\eta = \tan \bar{\delta}_b \tag{50}$$

$$\varpi = k_y + \left(1 - \tanh^2\left(\frac{y_e}{\sigma_1}\right)\right)\frac{\rho_1}{\sigma_1}. \tag{51}$$

Remark. For simplicity it is assumed that v_r is constant, in case v_r is time-varying, only variation is adding $\frac{\dot{v}_r}{v_r^2}\left(-k_y y_e + \hat{\bar{v}}_y - \rho_1 \tanh \frac{y_e}{\sigma_1}\right)$ in (49).

Step 2: consider the Lyapunov function as

$$V_2 = V_1 + \frac{1}{2}\tilde{u}_1^2 + \frac{1}{2}(\hat{\eta} - \eta)^T \gamma^{-1}(\hat{\eta} - \eta) \tag{52}$$

where γ is positive definite, $\hat{\eta}$ indicates the estimation of η. The time derivative of V_2 along (41) is

$$\begin{aligned}\dot{V}_2 &= x_e(-v_\omega - v_x^s + v_r \cos\theta_e) + y_e(v_r u_1 - \hat{\bar{v}}_y - \varepsilon_1) \\ &\quad + (\hat{\bar{v}}_y - \bar{v}_y)^T \Gamma^{-1}(\dot{\hat{\bar{v}}}_y + \Gamma y_e) + \tilde{u}_1\dot{\tilde{u}}_1 + (\hat{\eta} - \eta)^T \gamma^{-1}\dot{\hat{\eta}}.\end{aligned} \tag{53}$$

Substituting (43), (47) and (49) into (53), we have the following equation

$$\begin{aligned}\dot{V}_2 &\le -k_x x_e^2 - k_y y_e^2 - (\rho_1 - |\varepsilon_1|)|y_e| + y_e v_r \tilde{u}_1 \\ &\quad + (\hat{\bar{v}}_y - \bar{v}_y)^T \Gamma^{-1}(\dot{\hat{\bar{v}}}_y + \Gamma y_e) \\ &\quad + \tilde{u}_1\left(\cos\theta_e\left(c(s)v_r + \frac{\bar{v}_y + \varepsilon_1}{l}\right.\right. \\ &\quad \left.\left. - \frac{v_\omega + v_x^s}{l}(\tan\delta + \eta + \varepsilon_2)\right) + \frac{1}{v_r}(\varpi\dot{y}_e - \dot{\hat{\bar{v}}}_y)\right) \\ &\quad + (\hat{\eta} - \eta)^T \gamma^{-1}\dot{\hat{\eta}} + \zeta_1.\end{aligned} \tag{54}$$

In this equation regard $u_2 = \tan\delta$ as the virtual control input of the second step. From (54) the following equation can be obtained by algebraic transformation (see Appendix D or [26] for details)

$$\begin{aligned}\dot{V}_2 &\le -k_x x_e^2 - k_y y_e^2 - (\rho_1 - |\varepsilon_1|)|y_e| \\ &\quad + \tilde{u}_1\left(\lambda - \beta u_2 + \alpha - \frac{\varpi\varepsilon_1}{v_r} - \beta\hat{\eta} + \tau\varepsilon_1 - \beta\varepsilon_2\right) \\ &\quad + (\hat{\bar{v}}_y - \bar{v}_y)^T \Gamma^{-1}\left(\dot{\hat{\bar{v}}}_y + \Gamma y_e - \Gamma\tilde{u}_1\tau + \Gamma\frac{\varpi}{v_r}\tilde{u}_1\right) \\ &\quad + (\hat{\eta} - \eta)^T \gamma^{-1}(\dot{\hat{\eta}} + \gamma\tilde{u}_1\beta) + \zeta_1\end{aligned} \tag{55}$$

where

$$\alpha = \frac{\varpi(v_r \sin\theta_e - \hat{\bar{v}}_y) - \dot{\hat{\bar{v}}}_y}{v_r} \tag{56}$$

$$\tau = \frac{1}{l}\left(\cos\theta_e + \frac{\varpi x_e}{v_r}\right) \tag{57}$$

$$\beta = (v_\omega + v_x^s)\tau \tag{58}$$

$$\lambda = y_e v_r + \cos\theta_e c(s) v_r + \tau\hat{\bar{v}}_y. \tag{59}$$

In (55) let

$$\begin{aligned}\dot{\hat{\eta}} &= -\gamma\tilde{u}_1\beta \\ \dot{\hat{\bar{v}}}_y &= -\Gamma y_e + \Gamma\tilde{u}_1\tau - \Gamma\frac{\varpi}{v_r}\tilde{u}_1\end{aligned} \tag{60}$$

and choose u_2 as

$$\begin{aligned}u_2 = \frac{1}{\beta}&\left(k_u\tilde{u}_1 + \lambda + \alpha - \beta\hat{\eta}\right. \\ &+ \rho_1\left(\frac{\cos\theta_e}{l} + \frac{\varpi}{v_r}\left|\frac{x_e - l}{l}\right|\right)\tanh\left(\frac{\tilde{u}_1}{\sigma_2}\right) \\ &\left.+ |\beta|\rho_2\tanh\left(\frac{\tilde{u}^1}{\sigma_3}\right)\right)\end{aligned} \tag{61}$$

where $\sigma_i > 0$, then we get

$$\begin{aligned}\dot{V}_2 &\le -k_x x_e^2 - k_y y_e^2 - k_u\tilde{u}_1^2 - (\rho_1 - |\varepsilon_1|)|y_e| \\ &\quad - (\rho_2 - |\varepsilon_2|)|\beta||\tilde{u}_1| \\ &\quad - (\rho_1 - |\varepsilon_1|)\left(\frac{\cos\theta_e}{l} + \frac{\varpi}{v_r}\left|\frac{x_e - l}{l}\right|\right)|\tilde{u}_1| + \zeta\end{aligned} \tag{62}$$

where $\zeta = \zeta_1 + \zeta_2$, ζ_2 is another trivial variation due to the usage of tanh() instead of sign() in the variable structure controller (61). Note that $|\theta_e| < \frac{\pi}{2}$ and $\varpi > 0$, (62) implies that the closed-loop system is uniformly bounded.

4.2. Stability analysis

From (62) it is known that the longitudinal deviation x_e, lateral deviation y_e and $\tilde{u}_1$ are all bounded. Indeed all of them converge into a neighborhood of zero. The range of the neighborhood is determined by ζ which is linked to σ_i. The smaller σ_i is, the smaller the range of the neighborhood is, yielding higher accuracy.

When y_e and $\tilde{u}_1$ vary around zero, from (46) and (47) one gets that the orientation error θ_e converges into a neighborhood of

$$\theta_e = \arcsin\left(\frac{\hat{\bar{v}}_y}{v_r}\right). \tag{63}$$

5. Simplified adaptive controller with projection mapping

The robust adaptive controller (61) with VSC can guarantee high tracking accuracy from the academic point of view. However it needs a large amount of on-board computation and high-order derivatives of sign-like functions may make control inputs too oscillating.

To be of more advantage in actual applications, the robust adaptive controller is simplified by setting ρ_i to zero, then we get $\varpi = k_y$ and the controller (61) is reduced into an ordinary adaptive controller without VSC components.

$$u_2 = \frac{1}{\beta}(k_u\tilde{u}_1 + \lambda + \alpha - \beta\hat{\eta}). \tag{64}$$

By using the similar Lyapunov's direct method, it is proven that the adaptive controller (64) leads to the following result

$$\dot{V}_2 = k_x x_e^2 - k_y y_e^2 - k_u \tilde{u}_1^2 + \varepsilon_1 \left(\frac{\tilde{u}_1 \cos\theta_e}{l} - \frac{\tilde{u}_1 k_y}{v_r} - y_e \right) - \tilde{u}_1 \cos\theta_e \frac{v_x}{l} \varepsilon_2 \tag{65}$$

(65) implies the closed-loop system can be uniformly bounded by choosing (k_x, k_y, k_u). But comparing with (62) in which only ζ is a negligible disturbance, (65) is subjected to all the unmodeled sliding effects, leading to worse control performances than the robust adaptive controller (62).

To improve the control performances, projection mapping is used for the parameter adaptation procedure which makes the adaptive controller (64) robust to the unmodelled sliding effects. The projection mapping $\mathrm{Proj}_\xi(\bullet)$ is defined by [23,24]

$$\mathrm{Proj}_\xi(\bullet) = \begin{cases} 0 & \text{if } \hat{\xi} = \xi_{\max} \text{ and } \bullet > 0 \\ 0 & \text{if } \hat{\xi} = \xi_{\min} \text{ and } \bullet < 0 \\ \bullet & \text{otherwise.} \end{cases} \tag{66}$$

By using projection mapping $\mathrm{Proj}_\xi(\bullet)$, the robust adaptive laws become

$$\dot{\hat{\bar{v}}}_y = \mathrm{Proj}_{\bar{v}_y} \left(-\Gamma y_e + \Gamma \tilde{u}_1 \tau - \Gamma \frac{\varpi}{v_r} \tilde{u}_1 \right) \tag{67}$$

$$\dot{\hat{\eta}} = \mathrm{Proj}_\eta \left(-\gamma \tilde{u}_1 \beta \right). \tag{68}$$

The prior information on the bounds of the sliding effects $\bar{v}_y, \eta$ can be obtained off-line after performing large number of absolute coordinates measurements under different typical working conditions.

6. Simulation and experimental results

6.1. Simulation results

A classical "U" path with a perfect circular arc (path #1) is applied as the reference trajectory to test the proposed controllers. In the simulations, the gains used in (43) and (61) are set as $k_x = 0.6$, $k_y = 0.15$, $k_u = 1.14$. The gains of the adaptive laws (60) are set as $\Gamma = 0.2$, $\gamma = 0.05$. In actual implementations these gains should be tuned gradually to make an optimal compromise between transient characteristic and limited bandwidth of the steering system. The reference velocity is set as $v_r = 8.4$ km/h which is the normal velocity of the agriculture vehicles in agriculture applications.

In the simulation the constant sliding is introduced with $v_y = -0.1$, $\delta_b = -0.048$. The low-level delay of the steering system is considered. The control law (36), (37) without considering sliding is applied also with the same controller gains. The simulation results of the longitudinal, lateral and orientation errors are shown by Figs. 2–4. Since the vehicle velocity is initialized to zero, obvious longitudinal errors are noticed at the beginning of the simulations. The initial orientation errors are also nonzero. Those initial errors quite fit in with the real working conditions. From the simulations it is clear that all the controllers can make the longitudinal-lateral

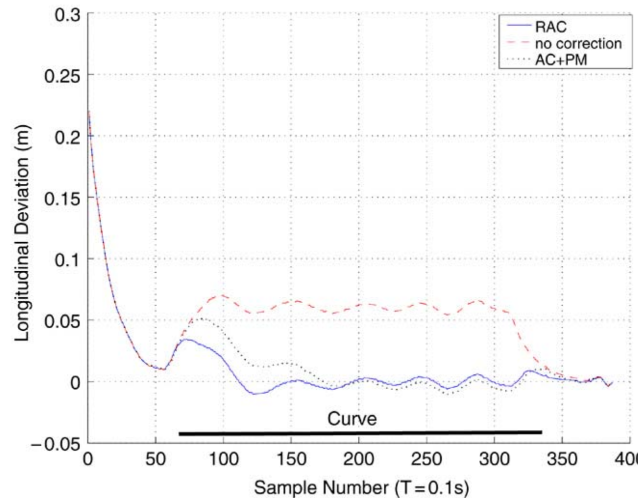

Fig. 2. Longitudinal deviation of path #1.

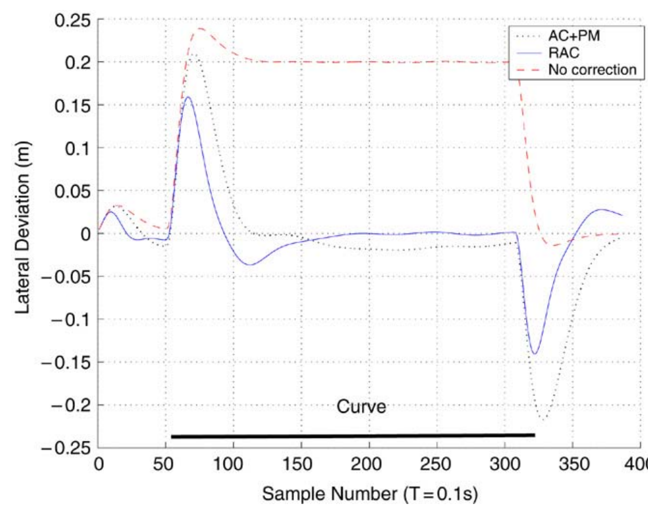

Fig. 3. Lateral deviation of path #1.

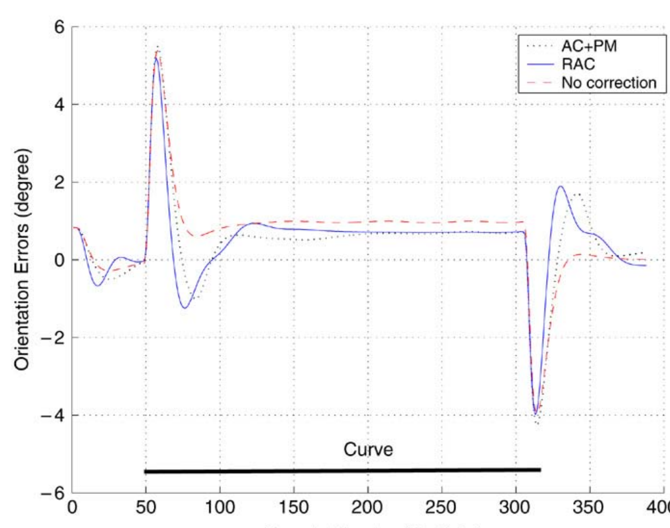

Fig. 4. Orientation errors of path #1.

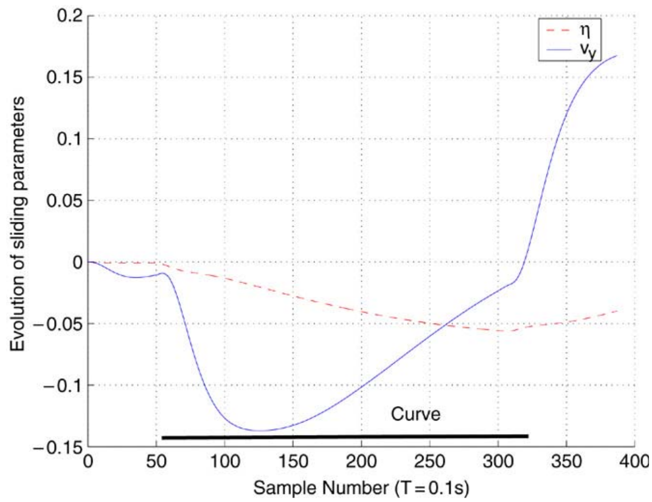

Fig. 5. Evolution of sliding parameters.

errors approach to zero before sliding occurs. But when sliding appears, because the control law (36), (37) does not take sliding effects into account, the longitudinal-lateral deviations (dashed line) become significant. While the robust adaptive controller (61) can compensate sliding effects through estimating them on line and counteract modeling inaccuracy (for example linearization inaccuracy) by VSC, so the longitudinal-lateral deviations can converge to zero with a good transient response (solid line). Finally the adaptive controller (64) is simulated also. (64) can compensate time-invariant sliding, hence its longitudinal-lateral deviations (dotted line) converge to zero with small offsets (due to linearization approximation in (14c)). The remarkable overshoots at the beginning and end of the curve are caused by sudden change of the sliding effects and low level delay. The bounded orientation errors are shown by Fig. 4. As analyzed by Section 4.2 the proposed controllers cannot make the orientation errors converge to zero, indeed they are bounded around (63). It is normal when sliding occurs known as “crab sliding”. The evolution of the sliding parameters $\hat{\bar{v}}_y$ (solid line), $\hat{\eta}$ (dashed line) is displayed by Fig. 5. At the beginning and end of the circle, $\hat{\bar{v}}_y$ varies greatly which explains the overshoots of the lateral deviation, but as the vehicle follows the circle, $\hat{\bar{v}}_y$ and $\hat{\eta}$ evolve smoothly close to the real values.

6.2. Experimental results

The guidance system has been implemented and succesfully tested on a CLAAS Dominator combine-harvester. The farm vehicle is depicted by Fig. 6. The GPS is Dassault-Sercel, dual frequency GPS 5002 system. This realtime kinematic carrier-phase differential GPS provides position and velocity measurements with a 2 cm accuracy, at a 10 Hz sampling frequency. The rotating velocity of the rear wheel was measured by optical rotary encoders. The actual front wheel angle was measured by means of absolute encoders and compared with its desired value. A PD algorithm implemented on a micro-processor controlled a electro-hydraulic valve. During all the experiments, the state vectors were constructed from the GPS data.

Fig. 6. Farm vehicle used in the experiment.

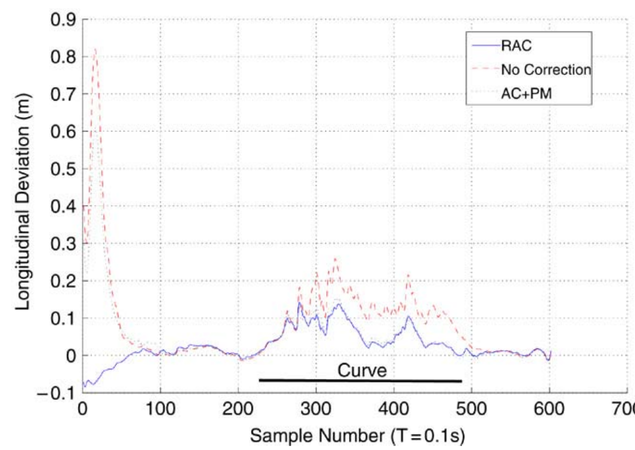

Fig. 7. Longitudinal deviation of experimental results.

Note that the control law is mostly related to the vehicle heading θ, unfortunately due to measurement noises and jounce of the GPS antenna mounted on the vehicle cabin ceiling, the computed orientation angle θ is very noisy. From an experimental point of view, this leads to very noisy and vibrating control signals. The low level system including the valves, are strongly actuated. Thanks to the Kalman reconstructor, in real experiments the heading was estimated. The same non-linear control law was still used. The reconstructed orientation angle is far smoother which leads to a comfortable behavior of the vehicle.

The control laws has been implemented in high level language (C++) on a Pentium based computer. A “U” path was followed. Each trial started with different initial conditions. The farm vehicle underwent sliding effects when it entered into a curve on a wet grass land. The longitudinal-lateral deviations are shown by Figs. 7 and 8. The actual deviations appear quite similar to those obtained in simulation. It can just be noticed that lateral deviation overshoots, at the beginning and at the end of the curve, are larger than those in simulation. It is because the presence of a filter introduces some delays. Moreover, delays introduced by low level actuators amplify also these overshoots. Nevertheless, it must be pointed out that the (robust) adaptive controllers can bring the vehicle back to the reference trajectory, they yield small lateral deviations with

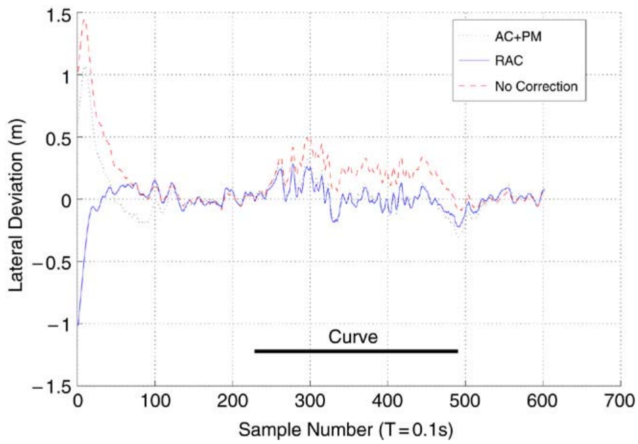

Fig. 8. Lateral deviation of experimental results.

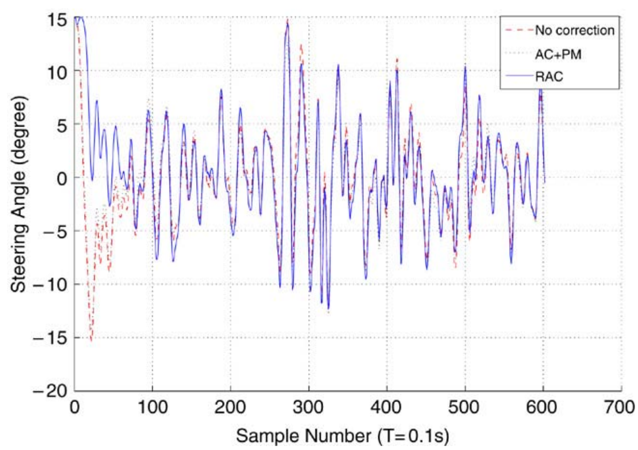

Fig. 9. Steering angle of the front wheel.

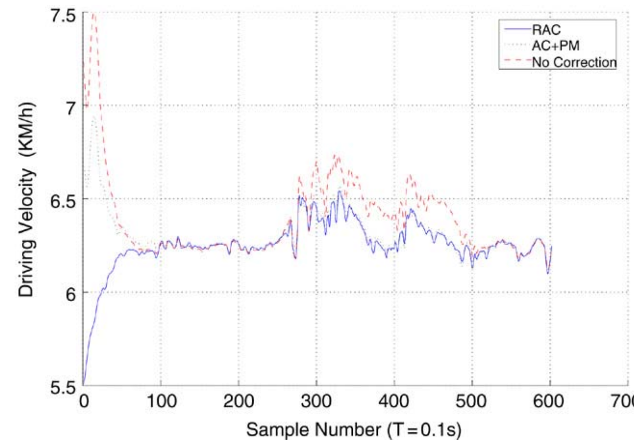

Fig. 10. Driving velocity of the rear wheel.

zero mean value during the curve. While the lateral deviation of the controller (37) is significant and has obvious bias. The longitudinal errors of the (robust) adaptive controllers are also less than that of (36). It is because when the lateral sliding and steering bias are compensated by the (robust) adaptive controllers, the negative influences of y_e and θ_e (due to sliding) on the longitudinal tracking accuracy are moderated.

The control inputs δ and v_ω of each controller are shown by Figs. 9 and 10. The robust adaptive controller with VSC yields good transient performances at the expense of strong control signals (solid line) and non-smooth movements. While the adaptive controller (64) with projection mapping yields a tracking movement with moderate control signals (dotted line), but its bias is larger than VSC's. So in case when sliding is dominant, the robust adaptive controller with VSC is favorable. But for the vehicles whose bandwidth is very limited, the adaptive controller with projection mapping is preferred.

7. Conclusion

The problem of trajectory tracking control of autonomous agricultural vehicles in the presence of sliding is investigated in this paper. A kinematic model which integrates the sliding effects as additive unknown parameters is constructed. From this model, a robust adaptive controller is designed based on backstepping methods which can stabilize the longitudinal-lateral derivations into a neighborhood of zero and guarantees the orientation error converge into a neighborhood near the origin. In addition a reduced adaptive controller with projection mapping is proposed for the purpose of smooth vehicle movements. Experimental comparative results show the effectiveness of the proposed control laws. The advantages of this scheme are that

- When no sliding occurs, the proposed controller can guarantee longitudinal-lateral deviations and orientation errors converge to zero.
- Integrating parameter adaptation with backstepping schemes yields a practical trajectory tracking controller for agriculture vehicles. The undertaking of sliding correction is shared between parameter adaptation and VSC. Also it is applicable for platoon control.
- Backstepping procedures can be extended easily to high-order nonholonomic systems, for example trailer control.

The prospective works include extending backstepping methods to platoon control and using predictive control to decrease overshoots of lateral deviations [25].

Appendix A

From (1) the following equation holds

$$\begin{cases} x_e = (x_r - x)\cos\theta + \sin\theta(y_r - y) \\ y_e = -(x_r - x)\sin\theta + \cos\theta(y_r - y). \end{cases} \tag{A.1}$$

Differentiating this equation we obtain that

$$\begin{cases} \dot{x}_e = (\dot{x}_r - \dot{x})\cos\theta - (x_r - x)\sin\theta\omega \\ \qquad + (\dot{y}_r - \dot{y})\sin\theta + (y_r - y)\cos\theta\omega \\ \dot{y}_e = -(\dot{x}_r - \dot{x})\sin\theta - (x_r - x)\cos\theta\omega \\ \qquad + (\dot{y}_r - \dot{y})\cos\theta - (y_r - y)\sin\theta\omega. \end{cases} \tag{A.2}$$

Under the pure rolling conditions, we have the following velocity constraints

$$\begin{cases} \dot{x}_r = v_r\cos\theta_r \\ \dot{y}_r = v_r\sin\theta_r \end{cases} \tag{A.3}$$

$$\begin{cases} \dot{x} = v\cos\theta \\ \dot{y} = v\sin\theta. \end{cases} \tag{A.4}$$

Substituting (A.3) and (A.4) into (A.2), we get

$$\begin{cases} \dot{x}_e = (v_r\cos\theta_r - v\cos\theta)\cos\theta - (x_r - x)\sin\theta\omega \\ \qquad + (v_r\sin\theta_r - v\sin\theta)\sin\theta + (y_r - y)\cos\theta\omega \\ \dot{y}_e = -(v_r\cos\theta_r - v\cos\theta)\sin\theta - (x_r - x)\cos\theta\omega \\ \qquad + (v_r\sin\theta_r - v\sin\theta)\cos\theta - (y_r - y)\sin\theta\omega. \end{cases} \tag{A.5}$$

After applying simple triangle transformation and considering (A.1) we obtain

$$\begin{cases} \dot{x}_e = -v + v_r\cos\theta_e + \omega y_e \\ \dot{y}_e = v_r\sin\theta_e - \omega x_e. \end{cases} \tag{A.6}$$

Appendix B

When sliding occurs, (A.1)–(A.3) still make sense, but the constraint (A.4) has to be refined by

$$\begin{cases} \dot{x} = v\cos(\theta + \varphi) \\ \dot{y} = v\sin(\theta + \varphi) \end{cases} \tag{B.1}$$

where φ is the side sliding angle. Then introducing (A.3) and (B.1) into (A.2) we obtain

$$\begin{cases} \dot{x}_e = (v_r\cos\theta_r - v\cos(\theta+\varphi))\cos\theta - (x_r - x)\sin\theta\omega \\ \qquad + (v_r\sin\theta_r - v\sin(\theta+\varphi))\sin\theta + (y_r - y)\cos\theta\omega \\ \dot{y}_e = -(v_r\cos\theta_r - v\cos(\theta+\varphi))\sin\theta - (x_r - x)\cos\theta\omega \\ \qquad + (v_r\sin\theta_r - v\sin(\theta+\varphi))\cos\theta - (y_r - y)\sin\theta\omega. \end{cases} \tag{B.2}$$

After performing simple algebra deduction we obtain

$$\begin{cases} \dot{x}_e = -v\cos\varphi + v_r\cos\theta_e + \omega y_e \\ \dot{y}_e = -v\sin\varphi + v_r\sin\theta_e - \omega x_e. \end{cases} \tag{B.3}$$

Due to the definition of (9) and (10), it is obvious that

$$\begin{cases} \dot{x}_e = -v_x + v_r\cos\theta_e + \omega y_e \\ \dot{y}_e = -v_y + v_r\sin\theta_e - \omega x_e. \end{cases} \tag{B.4}$$

Appendix C

The time derivative of (46) is

$$\dot{\tilde{u}}_1 = \dot{u}_1 - \dot{u}_{1d} = \cos\theta_e\dot{\theta}_e - \frac{-k_y\dot{y}_e + \dot{\hat{\bar{v}}}_y - \frac{\mathrm{d}}{\mathrm{d}t}\rho_1\tanh\left(\frac{y_e}{\sigma_1}\right)}{v_r}. \tag{C.1}$$

Consider the kinematic model of $\dot{\theta}_e$ with linearization approximation (14c), it is obtained that

$$\dot{\tilde{u}}_1 = \cos\theta_e\left(c(s)v_r + \frac{\bar{v}_y + \varepsilon_1}{l} - \frac{v_\omega + v_x^s}{l}(\tan\delta + \tan\bar{\delta}_b + \varepsilon_2)\right) - \frac{-k_y\dot{y}_e + \dot{\hat{\bar{v}}}_y - \frac{\rho_1}{\sigma_1}(1 - \tanh^2(\frac{y_e}{\sigma_1}))\dot{y}_e}{v_r}. \tag{C.2}$$

Define

$$\varpi = k_y + \left(1 - \tanh^2\left(\frac{y_e}{\sigma_1}\right)\right)\frac{\rho_1}{\sigma_1} \tag{C.3}$$

then we get

$$\dot{\tilde{u}}_1 = \cos\theta_e\left(c(s)v_r + \frac{\bar{v}_y + \varepsilon_1}{l} - \frac{v_\omega + v_x^s}{l}(\tan\delta + \tan\bar{\delta}_b + \varepsilon_2)\right) + \frac{\varpi\dot{y}_e - \dot{\hat{\bar{v}}}_y}{v_r}. \tag{C.4}$$

Appendix D

In Step 2 consider the Lyapunov function as

$$V_2 = V_1 + \frac{1}{2}\tilde{u}_1^2 + \frac{1}{2}(\hat{\eta} - \eta)^T\gamma^{-1}(\hat{\eta} - \eta). \tag{D.1}$$

The time derivative of V_2 along (41) is

$$\dot{V}_2 = x_e(-v_\omega - v_x^s + v_r\cos\theta_e) + y_e(v_r u_1 - \hat{\bar{v}}_y - \varepsilon_1) + (\hat{\bar{v}}_y - \bar{v}_y)^T\Gamma^{-1}(\dot{\hat{\bar{v}}}_y + \Gamma y_e) + \tilde{u}_1\dot{\tilde{u}}_1 + (\hat{\eta} - \eta)^T\gamma^{-1}\dot{\hat{\eta}}. \tag{D.2}$$

Here based on the backstepping schemes u_1 is replaced by $u_1 = u_{1d} + \tilde{u}_1$, then we obtain that

$$\dot{V}_2 = x_e(-v_\omega - v_x^s + v_r\cos\theta_e) + y_e(v_r u_{1d} - \hat{\bar{v}}_y - \varepsilon_1) + y_e v_r\tilde{u}_1 + (\hat{\bar{v}}_y - \bar{v}_y)^T\Gamma^{-1}(\dot{\hat{\bar{v}}}_y + \Gamma y_e) + \tilde{u}_1\dot{\tilde{u}}_1 + (\hat{\eta} - \eta)^T\gamma^{-1}\dot{\hat{\eta}}. \tag{D.3}$$

Substituting (43), (47) and (49) into (D.3) and considering (48), we have the following equation

$$\begin{aligned} \dot{V}_2 \le{}& -k_x x_e^2 - k_y y_e^2 - (\rho_1 - |\varepsilon_1|)|y_e| + y_e v_r\tilde{u}_1 \\ &+ (\hat{\bar{v}}_y - \bar{v}_y)^T\Gamma^{-1}(\dot{\hat{\bar{v}}}_y + \Gamma y_e) \\ &+ \tilde{u}_1\left[\cos\theta_e\left(c(s)v_r + \frac{\bar{v}_y + \varepsilon_1}{l} - \frac{v_\omega + v_x^s}{l}(\tan\delta + \eta + \varepsilon_2)\right) + \frac{1}{v_r}(\varpi\dot{y}_e - \dot{\hat{\bar{v}}}_y)\right] + (\hat{\eta} - \eta)^T\gamma^{-1}\dot{\hat{\eta}} + \zeta_1. \end{aligned} \tag{D.4}$$

Introducing expression of $\dot{y}_e$ of (14b) into (D.4), we have

$$\begin{aligned} \dot{V}_2 \le{}& -k_x x_e^2 - k_y y_e^2 - (\rho_1 - |\varepsilon_1|)|y_e| \\ &+ (\hat{\bar{v}}_y - \bar{v}_y)^T\Gamma^{-1}(\dot{\hat{\bar{v}}}_y + \Gamma y_e) \\ &+ \tilde{u}_1 y_e v_r + \tilde{u}_1\cos\theta_e\left[c(s)v_r + \frac{\bar{v}_y + \varepsilon_1}{l} - \frac{v_\omega + v_x^s}{l}(\tan\delta + \eta + \varepsilon_2)\right] \\ &+ \tilde{u}_1\frac{\varpi(v_r\sin\theta_e - (\bar{v}_y + \varepsilon_1)) - \dot{\hat{\bar{v}}}_y}{v_r} - \tilde{u}_1\varpi\frac{\omega x_e}{v_r} \\ &+ (\hat{\eta} - \eta)^T\gamma^{-1}\dot{\hat{\eta}} + \zeta_1. \end{aligned} \tag{D.5}$$

In (D.5), the angular velocity ω is substituted by the linearized kinematic model (14c). δ which is the steering angle of the front wheel is one of the control inputs, so we regard $u_2 = \tan\delta$ as the virtual control input of the Step 2.

$$\begin{aligned}\dot{V}_2 \le{}& -k_x x_e^2 - k_y y_e^2 - (\rho_1 - |\varepsilon_1|)|y_e| \\ &+ (\hat{\bar{v}}_y - \bar{v}_y)^T \Gamma^{-1}(\dot{\hat{\bar{v}}}_y + \Gamma y_e) \\ &+ \tilde{u}_1 y_e v_r + \tilde{u}_1 \cos\theta_e \left[c(s) v_r + \frac{\bar{v}_y + \varepsilon_1}{l} \right. \\ &\left. - \frac{v_\omega + v_x^s}{l}(u_2 + \eta + \varepsilon_2) \right] \\ &+ \tilde{u}_1 \frac{\varpi(v_r \sin\theta_e - (\bar{v}_y + \varepsilon_1)) - \dot{\hat{\bar{v}}}_y}{v_r} \\ &- \frac{\tilde{u}_1 \varpi x_e}{v_r}\left[\frac{v_\omega + v_x^s}{l}(u_2 + \eta + \varepsilon_2) - \frac{\bar{v}_y + \varepsilon_1}{l}\right] \\ &+ (\hat{\eta} - \eta)^T \gamma^{-1} \dot{\hat{\eta}} + \zeta_1. \end{aligned} \tag{D.6}$$

(D.6) is equivalent to the following equation in which $\hat{\bar{v}}_y$ (the estimation of $\bar{v}_y$) and $\hat{\eta}$ (the estimation of η) are introduced.

$$\begin{aligned}\dot{V}_2 \le{}& -k_x x_e^2 - k_y y_e^2 - (\rho_1 - |\varepsilon_1|)|y_e| \\ &+ (\hat{\bar{v}}_y - \bar{v}_y)^T \Gamma^{-1}(\dot{\hat{\bar{v}}}_y + \Gamma y_e) \\ &+ \tilde{u}_1 y_e v_r + \tilde{u}_1 \cos\theta_e \left[c(s) v_r + \frac{\bar{v}_y + \hat{\bar{v}}_y - \hat{\bar{v}}_y + \varepsilon_1}{l} \right. \\ &\left. - \frac{v_\omega + v_x^s}{l}(u_2 + \eta + \hat{\eta} - \hat{\eta} + \varepsilon_2) \right] \\ &+ \tilde{u}_1 \frac{\varpi(v_r \sin\theta_e - (\bar{v}_y + \hat{\bar{v}}_y - \hat{\bar{v}}_y + \varepsilon_1)) - \dot{\hat{\bar{v}}}_y}{v_r} \\ &- \frac{\tilde{u}_1 \varpi x_e}{v_r}\left[\frac{v_\omega + v_x^s}{l}(u_2 + \eta + \hat{\eta} - \hat{\eta} + \varepsilon_2) \right. \\ &\left. - \frac{\bar{v}_y + \hat{\bar{v}}_y - \hat{\bar{v}}_y + \varepsilon_1}{l}\right] + (\hat{\eta} - \eta)^T \gamma^{-1} \dot{\hat{\eta}} + \zeta_1. \end{aligned} \tag{D.7}$$

Then (D.7) can be transformed into the following equation

$$\begin{aligned}\dot{V}_2 \le{}& -k_x x_e^2 - k_y y_e^2 - (\rho_1 - |\varepsilon_1|)|y_e| \\ &+ (\hat{\bar{v}}_y - \bar{v}_y)^T \Gamma^{-1}(\dot{\hat{\bar{v}}}_y + \Gamma y_e) \\ &+ \tilde{u}_1 \left[y_e v_r + \cos\theta_e c(s) v_r - \left(\frac{\varpi x_e}{v_r} + \cos\theta_e\right) \right. \\ &\left. \times \frac{v_\omega + v_x^s}{l} u_2 \right] \\ &+ \tilde{u}_1 \left(\cos\theta_e + \frac{\varpi x_e}{v_r}\right)\frac{\hat{\bar{v}}_y + \varepsilon_1}{l} \\ &+ \tilde{u}_1 \frac{\varpi(v_r \sin\theta_e - \hat{\bar{v}}_y) - \dot{\hat{\bar{v}}}_y - \varpi\varepsilon_1}{v_r} \\ &+ \tilde{u}_1 \left(\cos\theta_e + \frac{\varpi x_e}{v_r}\right)\frac{\bar{v}_y - \hat{\bar{v}}_y}{l} \\ &- \tilde{u}_1 \left(\cos\theta_e + \frac{\varpi x_e}{v_r}\right)\frac{v_\omega + v_x^s}{l}(\hat{\eta} + \varepsilon_2) \\ &- \tilde{u}_1 \left(\cos\theta_e + \frac{\varpi x_e}{v_r}\right)\frac{v_\omega + v_x^s}{l}(\eta - \hat{\eta}) \\ &- (\bar{v}_y - \hat{\bar{v}}_y)\frac{\varpi \tilde{u}_1}{v_r} + (\hat{\eta} - \eta)^T \gamma^{-1} \dot{\hat{\eta}} + \zeta_1. \end{aligned} \tag{D.8}$$

By defining the following variables

$$\alpha = \frac{\varpi(v_r \sin\theta_e - \hat{\bar{v}}_y) - \dot{\hat{\bar{v}}}_y}{v_r} \tag{D.9}$$

$$\tau = \frac{1}{l}\left(\cos\theta_e + \frac{\varpi x_e}{v_r}\right) \tag{D.10}$$

$$\beta = (v_\omega + v_x^s)\tau \tag{D.11}$$

$$\lambda = y_e v_r + \cos\theta_e c(s) v_r + \tau \hat{\bar{v}}_y \tag{D.12}$$

we can obtain the following simplified form

$$\begin{aligned}\dot{V}_2 \le{}& -k_x x_e^2 - k_y y_e^2 - (\rho_1 - |\varepsilon_1|)|y_e| \\ &+ \tilde{u}_1 \left[\lambda - \beta u_2 + \alpha - \frac{\varpi\varepsilon_1}{v_r} - \beta\hat{\eta} + \tau\varepsilon_1 - \beta\varepsilon_2\right] \\ &+ (\hat{\bar{v}}_y - \bar{v}_y)^T \Gamma^{-1}\left(\dot{\hat{\bar{v}}}_y + \Gamma y_e - \Gamma \tilde{u}_1 \tau + \Gamma \frac{\varpi \tilde{u}_1}{v_r}\right) \\ &+ (\hat{\eta} - \eta)^T \gamma^{-1}(\dot{\hat{\eta}} + \gamma \tilde{u}_1 \beta) + \zeta_1. \end{aligned} \tag{D.13}$$

In (D.13) let

$$\begin{aligned}\dot{\hat{\eta}} &= -\gamma \tilde{u}_1 \beta \\ \dot{\hat{\bar{v}}}_y &= -\Gamma y_e + \Gamma \tilde{u}_1 \tau - \Gamma \frac{\varpi}{v_r}\tilde{u}_1. \end{aligned} \tag{D.14}$$

Then we can obtain

$$\begin{aligned}\dot{V}_2 \le{}& -k_x x_e^2 - k_y y_e^2 - (\rho_1 - |\varepsilon_1|)|y_e| + \zeta_1 \\ &+ \tilde{u}_1 \left[\lambda - \beta u_2 + \alpha - \beta\hat{\eta} + \left(\frac{\cos\theta_e}{l} \right.\right. \\ &\left.\left. + \frac{\varpi}{v_r}\frac{x_e - l}{l}\right)\varepsilon_1 - \beta\varepsilon_2\right]. \end{aligned} \tag{D.15}$$

Because it has been assumed that ε_i is bounded by ρ_i, it is straightforward to design u_2 as a variable structure controller

$$\begin{aligned} u_2 = \frac{1}{\beta}&\left(k_u \tilde{u}_1 + \lambda + \alpha - \beta\hat{\eta}\right. \\ &+ \rho_1\left(\frac{\cos\theta_e}{l} + \frac{\varpi}{v_r}\left|\frac{x_e - l}{l}\right|\right)\tanh\left(\frac{\tilde{u}_1}{\sigma_2}\right) \\ &\left.+ |\beta|\rho_2 \tanh\left(\frac{\tilde{u}_1}{\sigma_3}\right)\right). \end{aligned} \tag{D.16}$$

In the controller (D.16), the variable structure term $|\beta|\rho_2 \tanh(\frac{\tilde{u}_1}{\sigma_3})$ is used to counteract the negative effects of $\beta\varepsilon_2$. Moreover another variable structure term $\rho_1\left(\frac{\cos\theta_e}{l} + \frac{\varpi}{v_r}|\frac{x_e - l}{l}|\right)$ $\tanh(\frac{\tilde{u}_1}{\sigma_2})$ is designed to counteract the negative effects of $(\frac{\cos\theta_e}{l} + \frac{\varpi}{v_r}\frac{x_e - l}{l})\varepsilon_1$. So we finally achieve the Lyapunov result of (62).

References

[1] T.S. Stombaugh, Automatic guidance of agricultural vehicles at higher speeds, Ph.D. Dissertation, Dept. of Agriculture Engineering, University of Illinois at Urbana-Champaign, 1997.
[2] Z.-P. Jiang, H. Nijmeijer, Tracking control of mobile robots: A case study inbackstepping, Automatica 33 (7) (1998) 1393–1399.
[3] J. Billingsley, M. Schoenfisch, Vision-guidance of agricultural vehicles, Autonomous Robots 2 (1995) 65–76.
[4] P. Morin, C. Samson, Application of backstepping techniques to the time-varying exponential stabilization of chained form systems, Technical Report 2792, INRIA Sophia Antipolis, 1996.
[5] A.A.J. Lefeber, Tracking control of nonlinear mechanical systems, Ph.D. Thesis, Universiteit Twente, 2000.
[6] G. Elkaim, M. O'Conner, T. Bell, B. Parkinson, System identification and robust control of farm vehicles using CDGPS, in: IONGPS-97, vol. 2, Kansas City, MO, USA, 1997, pp.1415–1424.
[7] J. Wit, Vector pursuit path tracking for autonomous ground vehicles, Ph.D. Dissertation, University of Florida, 2000.
[8] J. Ackermann, Robust control prevents car skidding, IEEE Control Systems Magazine (June) (1997) 23–31.
[9] C. Samson, Control of chained systems, application to path following and time-varying point stabilization of mobile robot, IEEE Transactions on Automatic Control 39 (12) (1995) 2411–2425.
[10] I. Motte, H. Campion, Control of sliding mobile robots: A slow manifold approach, MNTS, 2000.
[11] W. Leroquais, B. D'Andrea-Novel, Vibrational control of wheeled mobile robots not satisfying ideal velocity constraints: The unicycle case, in: European Control Conference, Brussels, 1–4 July 1997.
[12] Y.L. Zhang, J.H. Chung, S.A. Velinsky, Variable structure control of a differentially steered wheeled mobile robot, Journal of Intelligent and Robotic Systems 36 (2003) 301–314.
[13] H. Fang, R. Lenain, B. Thuilot, P. Martinet, Sliding mode control of automatic guidance of farm vehicles in the presence of sliding, in: The 4th International Symposium on Robotics and Automation, Queretaro, Mexico, August 2004, pp. 582–587.
[14] M.L. Corradini, G. Orlando, Experimental testing of a discrete-time sliding mode controller for trajectory tracking of a wheeled mobile robot in the presence of skidding effects, Journal of Robotic Systems 19 (4) (2002) 177–188.
[15] B. D'Andrea-Novel, G. Campion, G. Bastin, Control of wheeled mobile robots not satisfying ideal constraints: A singular perturbation approach, International Journal of Robust Nonlinear Control 5 (1995) 243–267.
[16] R. Lenain, B. Thuilot, C. Cariou, P. Martinet, Adaptive control for car like vehicles guidance relying on RTK GPS: Rejection of sliding effects in agricultural applications. in: Proc. of the Intern. Conf. On Robotics and Automation, Taipei, September 2003, pp. 115–120.
[17] H. Fang, R. Lenain, B. Thuilot, P. Martinet, Robust adaptive control of automatic guidance of farm vehicles in the presence of sliding, in: IEEE International Conference on Robotics and Automation, Barcelona, 18–22 April 2005, pp. 3113–3118.
[18] Z.P. Jiang, H. Nijmeijer, A recursive technique for tracking control of nonholonomic systems in chained form, IEEE Transactions on Automatic Control 44 (2) (1999) 265–279.
[19] R. Marino, P. Tomei, Nonlinear Control Design, Prentice-Hall, Hemel Hempstead Hertfordshire, England, 1995.
[20] M. Krstic, I. Kanellakopoulos, P.V. Kokotovic, Nonlinear and Adaptive Control Design, John Wiley and Sons, ISBN: 0-471-12732-9, 1995.
[21] Y.P. Zhang, B. Fidan, P.A. Ioannou, Backstepping control of linear time-varying systems with known and unknown parameters, IEEE Transactions on Automatic Control 48 (2003) 1908–1925.
[22] R. Brockett, Control Theory and Singular Riemannian Geometry. New Directions in Applied Mathematics, Springer, Berlin, 1981.
[23] B. Yao, M. Tomizuka, Smooth robust adaptive sliding mode control of robot manipulators with guaranteed transient performance, Transactions of the ASME, Journal of Dynamic Systems, Measurement and Control 118 (4) (1996) 764–775.
[24] S. Sastry, M. Bodson, Adaptive Control: Stability, Convergence, and Robustness, Prentice-Hall, ISBN: 0-13-004326-5, 1989.
[25] R. Lenain, B. Thuilot, C. Cariou, P. Martinet, Model predictive control of vehicle in presence of sliding application to farm vehicles path tracking, in: IEEE International Conference on Robotics and Automation, Barcelona, 18–22 April 2005, pp. 897–902.
[26] H. Fang Automatic guidance of farm vehicles in the presence of sliding, Scientific Reports of LASMEA, http://srvlas.univ-bpclermont.fr/Control/index.html, 2004.

H. Fang received his Ph.D. Diploma from Xi'an Jiaotong University in 2002. He held two postdoctoral appointments at INRIA/France research group of COPRIN and at LASMEA (UNR6602 CNRS/Blaise Pascal University, Clermont-Ferrand, France). Since 2005 he has been an assistant professor at Beijing Institute of Technology. His research interests include all-terrain mobile robots, robotic control and parallel manipulators.

Ruixia Fan has been a full professor at Beijing Institute of Technology since 2003. Her research interests include intelligent systems, pattern recognition and visual servoing.

B. Thuilot received his Electrical Engineer and Ph.D. Diploma in 1991 and 1995. He held postdoctoral appointment at INRIA research units of Grenoble, France (1996) and of Sophia-Anitpolis, France (1997). Since 1997 he has been an assistant professor at Blaise Pascal University of Clermont-Ferrand, France. He is also a research scientist at LASMEA-CNRS Lab. His research interests include nonlinear control of mechanical systems, with application to vehicle and to high speed manipulators with parallel kinematics.

P. Martinet received his Electrical Engineer and Ph.D. Diploma in 1985 and 1987. He spent three years in the Electrical industry. From 1990 to 2000, he was an assistant professor at CUST University of Clermont-Ferrand, France. Since 2000, he has been a full professor at IFMA/France. Since 1990 he has also been a research scientist at LASMEA-CNRS. His research interests include automatic guided vehicles, active vision and sensor integration, visual servoing and parallel architecture for visual servoing applications.